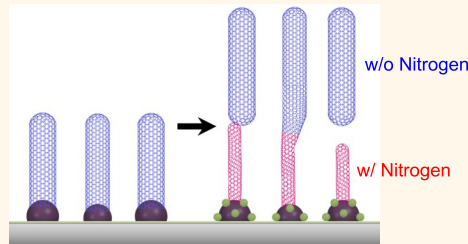


Reversible Diameter Modulation of Single-Walled Carbon Nanotubes by Acetonitrile-Containing Feedstock

Teerapol Thurakitseree,[†] Christian Kramberger,[‡] Akihito Kumamoto,[§] Shohei Chiashi,[†] Erik Einarsson,^{†,⊥} and Shigeo Maruyama^{†,*}

[†]Department of Mechanical Engineering, [§]Institute of Engineering Innovation School of Engineering, and [⊥]Global Center of Excellence for Mechanical Systems Innovation, The University of Tokyo, 7-3-1 Hongo, Bunkyo-ku, Tokyo 113-8656, Japan, and [‡]Faculty of Physics, University of Vienna, Strudlhofgasse 4, Vienna, A-1090, Austria

ABSTRACT Changing the carbon feedstock from pure ethanol to a 5 vol % mixture of acetonitrile in ethanol during the growth of vertically aligned single-walled carbon nanotubes (SWNTs) reduces the mean diameter of the emerging SWNTs from approximately 2 to 1 nm. We show this feedstock-dependent change is reversible and repeatable, as demonstrated by multilayered vertically aligned SWNT structures. The reversibility of this process and lack of necessity for catalyst modification provides insight into the role of nitrogen in reducing the SWNT diameter.



KEYWORDS: vertically aligned · single-walled carbon nanotube · SWNT · doped SWNT · diameter control · acetonitrile

The properties of single-walled carbon nanotubes (SWNTs) are strongly dependent on their structure, and typically become more enhanced as the nanotube diameter decreases. As a result, chirality and diameter control—particularly during synthesis—offers great potential for tuning the properties of SWNTs. It is widely accepted that the SWNT diameter is largely determined by the size of the catalyst nanoparticle, and this size relationship has been thoroughly studied.^{1–9} Because of this relationship, there have been many attempts to reduce the SWNT diameter by reducing the catalyst particle size. SWNTs with diameters in the range of 0.6–1.1 nm have been synthesized by impregnating SiO₂ particles with Co/Mo.^{3,5,10} A similar selectivity has been obtained using Co/Fe,^{8,11} Fe/MgO,¹² and Co incorporated into MCM-411.¹³ These methods, however, require the use of a powder, mesoporous material. Separating the SWNTs from the support requires significant postprocessing, which can alter the SWNT properties.

Several methods to alter the SWNT structure during growth have also been demonstrated by changing growth temperature,^{1,8} and/or pressure.^{14,15} Changes in diameter along a nanotube axis due to rapidly changing

temperature have been previously reported for individual SWNTs,¹⁶ DWNTs,¹⁷ and other configurations of intramolecular junctions.^{18–23} There are fewer studies on the influence of the precursor, but SWNT diameters have been found to be sensitive to abrupt changes in feedstock flux.^{24–26} Tian *et al.*²⁷ recently demonstrated successful control over the diameter in the range of 1.2–1.9 nm by adjusting CO₂ concentration. Selectivity of diameter and chiral angle have also been shown by selective etching.^{28–31} We have previously reported that incorporating acetonitrile (CH₃CN) into the ethanol feedstock results in a reduction of mean SWNT diameter from 2.1 nm to less than 1 nm,^{32,33} but the role of nitrogen in this diameter change is not yet understood.

In this study, we demonstrate *reversible* diameter modulation of vertically aligned SWNTs (VA-SWNTs) by adding acetonitrile to the feedstock during synthesis by alcohol catalytic chemical vapor deposition (CVD). This change was observed regardless of the sequence in which the carbon feedstocks were introduced. On the basis of this reversibility, investigation of the layer interface, and our previous findings, we put forward an explanation of nitrogen's role in reducing the diameter of SWNTs.

* Address correspondence to maruyama@photon.t.u-tokyo.ac.jp.

Received for review November 7, 2012 and accepted February 26, 2013.

Published online March 07, 2013
10.1021/nn3051852

© 2013 American Chemical Society

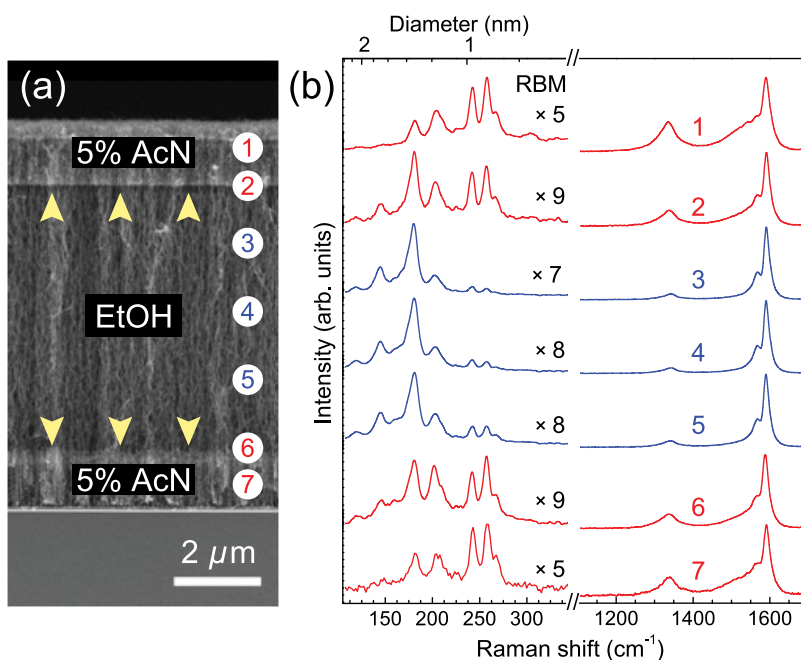


Figure 1. Reversibility of SWNT diameter demonstrated by growth of a triple-layered SWNT array characterized by SEM (a) and 488 nm resonance Raman spectra (b). The yellow arrows in panel a denote the interfaces between different SWNT layers.

RESULTS AND DISCUSSION

Reversible and Repeatable Diameter Modulation. To determine whether or not the diameter of SWNTs within the same array can be modulated by changing the feedstock we split the growth into multiple stages as follows. We first initiated VA-SWNT synthesis using 5 vol % acetonitrile in ethanol (5% AcN). After 2 min of synthesis we stopped the feedstock supply for 90 s, then supplied pure ethanol (EtOH) into the CVD chamber. After exposure to ethanol for 90 s, we again stopped the supply and changed the feedstock back to 5% AcN. A scanning electron microscope (SEM) image showing a cross-section of the resulting array is shown in Figure 1a. The VA-SWNT array is composed of three layers, with the interface between layers (indicated by arrows) appearing as a change in contrast in the SEM image. Since the formation of VA-SWNTs is known to be a root-growth process³⁴ the upper part of the array is formed first, and the part nearest the substrate is formed last.

Resonance Raman spectra were obtained at several points along the height of the array, with the approximate positions indicated by the circles numbered 1–7 in Figure 1a. Raman spectra corresponding to these positions are shown in Figure 1b. The very different spectra along the array indicate the layers are comprised of very different nanotubes. Spectra obtained from the central region (points 3, 4, and 5) are typical of ethanol-grown VA-SWNTs (Et-SWNTs), whereas the spectra obtained from regions above and below

(points 1, 2, 7, and 8) are remarkably similar to those grown from 5% AcN (Ac-SWNTs).³²

The low-energy radial breathing mode (RBM) peaks originate from SWNTs of a specific chirality that are in resonance with the excitation laser (here, 488 nm), and the frequency of this mode is known to have a clear diameter dependence.^{35,36} A corresponding diameter scale is shown on the upper axis in the RBM region of Figure 1b. We used the empirical relation³⁷ $\omega_{\text{RBM}} = 217.8/d + 15.7$ to estimate the tube diameter, where ω_{RBM} is the Raman shift in cm^{-1} and d is the tube diameter in nm. Peaks from larger-diameter semiconducting Et-SWNTs at 145 and 160 cm^{-1} originate from resonances of third (E_{33}^S) and fourth order (E_{44}^S) optical transitions, whereas peaks at 245 and 265 cm^{-1} originate from a resonance of the excitation laser with the first optical transition of small-diameter metallic SWNTs (E_{11}^M).

The SWNTs grown in the presence of 5% acetonitrile (Ac-SWNT) exhibit an increased D-line intensity (near 1350 cm^{-1}). This is a common characteristic when N is incorporated into the nanotubes.^{38,39} By contrast, the SWNTs grown from pure ethanol (Et-SWNTs) exhibit a much weaker D-line. The G-line (1500–1600 cm^{-1}) shows an increasing intensity of the Breit–Wigner–Fano (BWF) line shape for Ac-SWNTs, indicating an increased resonance with metallic SWNTs. This is corroborated by the appearance of intense RBM peaks from metallic SWNTs.

On the basis of the RBM spectra in Figure 1b, the layers containing Ac-SWNTs appear to have considerably smaller diameters than the Et-SWNT layer.

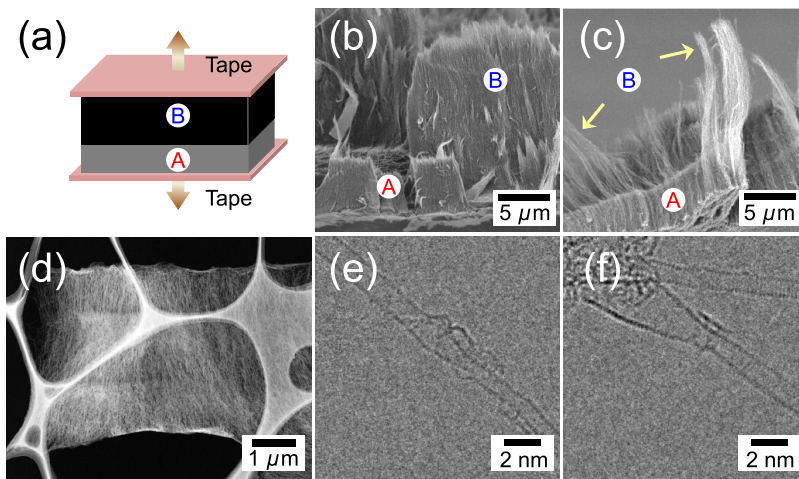


Figure 2. Interface examination (a) and SEM images of SWNT arrays synthesized, respectively, from 5% AcN and EtOH (b) in which the top layer was attached to adhesive tape before detaching the bottom layer with some continuous nanotubes indicated by yellow arrows (c); LAADF-STEM image of five layers array (d) with observable nanotube junctions between small- and large-diameter SWNTs observed from the interface region by HRTEM (e, f).

The strong presence of RBM peaks associated with small-diameter SWNTs for the 5% AcN case—and the absence of these peaks in the EtOH case—is strong evidence for diameter reduction. The RBM peaks in the resonance Raman spectra of double-layered VA-SWNTs (Supporting Information, Figures S1 and S2) also reveal a similarity of multilayered SWNTs and single arrays of as-grown *Et*- and Ac-SWNTs (Supporting Information, Figure S3,a–c). Resonance Raman spectra of the 2D (G') line obtained using the same 488 nm excitation wavelength (Supporting Information, Figure S3,d–f), were decomposed using two Voigtian peaks at 2620 and 2666 cm^{-1} for EtOH-grown SWNTs, and three Voigtian peaks at 2610, 2650, and 2680 cm^{-1} for 5% AcN-grown SWNTs. All peak components (black solid lines) were fitted with a constant full-width at half-maximum (FWHM) of 19.7 cm^{-1} . Supporting Information, Figure S3 panels d–f show identical G' spectra in all cases at the position of 2666 cm^{-1} for EtOH-grown SWNTs, and at 2610 cm^{-1} for 5% AcN-grown SWNTs. A large downshift is due to the vast difference in SWNT diameter, which has been observed in previous studies on N-doped SWNTs.^{32,40,41} These data clearly show that Ac-SWNTs and *Et*-SWNTs maintain their characteristic diameter distribution, regardless of the sequence of feedstock introduction.

While the Raman spectra of the double-layered arrays are consistent with those shown in an earlier report in which we confirmed the significant diameter reduction when using acetonitrile,³² we acknowledge that the mean diameter and diameter distribution cannot be rigorously determined only from these spectra. Therefore, we performed transmission electron microscope (TEM) observations on the different layers of a double-layered sample (Supporting Information, Figure S1) in which EtOH was introduced first, followed by 5% AcN. Diameter

measurements made from the images indicate a reduction in mean diameter from 1.66 ± 0.46 nm to 1.14 ± 0.40 nm when the feedstock was changed from EtOH to 5% AcN (see Supporting Information, Figure S4).

Investigating the Role of Nitrogen. To determine the role of nitrogen, we must examine what happens at the interface between the layers. Several previous studies of multilayered SWNT growth have reported that two different layers of carbon nanotubes^{42–44} are very weakly connected at the interface. We examined the strength of the interlayer connection by detaching the top layer of a double-layered array from the bottom layer using adhesive tape. We removed the entire array from the growth substrate by attaching tape to the top surface of the array (Ac-SWNTs, A) and peeling the array away from the substrate. Another piece of tape was then attached to the bottom surface of the array (*Et*-SWNTs, B), and the two pieces were then separated. SEM images obtained after separation are shown in Figures 2a–c. As seen in the figures, most of the layers cleanly separated from each other, indicating that the majority of SWNTs are not connected at the interface. However, some areas remained connected (indicated by arrows in Figure 2c), suggesting some of the SWNTs could be continuous through the interface.

A 5 μm , five-layer SWNT array was synthesized for interface examination (see Supporting Information, Figures S5,S6). Its low-angle annular dark-field STEM (LAADF-STEM) image is depicted in Figure 2d in which the interface can be clearly seen. Figure 2 panels e and f show high-resolution TEM (HRTEM) images of five-layer arrays obtained from the interface region (Supporting Information, Figure S7). These images clearly show a nanotube changing diameter from 1.2 to 0.8 nm in panel e, and from 2.4 to 1.1 nm in panel f.

Although statistics could not be performed regarding the frequency of junctions due to the entanglement of nanotubes at the interface, these observations demonstrate some SWNTs can be connected across the interface.

As previously mentioned, abrupt changes in growth conditions such as temperature^{16,17} and feedstock flux^{24–26} have been reported to induce continuous junctions in SWNTs and DWNTs. While the temperature was unchanged in the experiments reported here, the presence of nitrogen may have altered the flux of carbon into the catalyst. It has been shown that the mean diameter of SWNTs grown from ethanol is dependent on the precursor supply,^{9,45} but the sensitivity is not enough to explain the findings reported here based on the availability of carbon. We suspect, however, that nitrogen acts only at the catalyst surface, disrupting the SWNT formation. It is well-established that incorporation of nitrogen will easily induce defects into the SWNT structure,⁴⁶ and density functional theory (DFT) calculations⁴⁷ have shown that the binding energy between Co and N is higher than between Co and C. This means any nitrogen present on the catalyst will be less mobile than the surrounding carbon. This condition has been predicted to result in narrower SWNTs.⁴⁸

Fiawoo *et al.*⁴⁹ recently proposed that SWNT formation occurs near the edge of a catalyst particle when the growth condition is near thermodynamic equilibrium. This is called a “tangential” growth mode and explains why the diameter of a SWNT is typically dependent on the catalyst particle size. This also explains the gradual increase of mean diameter that typically results from increasing the growth temperature.^{9,16,17,50,51} Away from thermodynamic equilibrium, a “perpendicular” growth mode is possible, in which the SWNT diameter is independent of the catalyst particle size. These growth modes have been studied by *in situ* TEM observation.^{49,52} Fiawoo *et al.* proposed that nucleation occurs primarily by the perpendicular mode, which is dominant during the early stage of nanotube growth. After nucleation and the growth process approaches equilibrium, the tangential mode becomes dominant and remains so until growth stops.

Considering our experimental findings in light of the available literature, we propose that the diameter change caused by the presence of nitrogen is due to a process at the catalyst surface that causes a change from the tangential to the perpendicular growth mode. We rule out formation of a nitride with the metal catalyst because that is unlikely to be reversible. Furthermore, the production of N₂ during synthesis⁵³ suggests a mechanism by which nitrogen could often leave the catalyst, thereby being reversible. Moreover, a process which only occurs at the catalyst surface helps explain why a small percentage of nitrogen can have a significant effect.

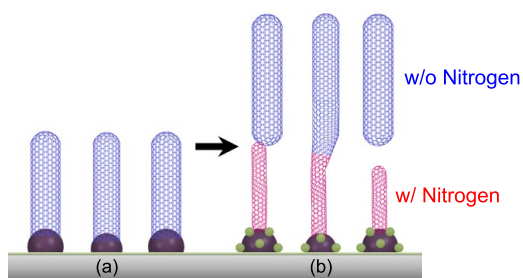


Figure 3. A possible mechanism of diameter change along VA-SWNT array from Co catalyst nanoparticles (a) without and (b) with N (green ball). Blue and red tubes represent larger and smaller SWNTs synthesized from ethanol (EtOH) and 5 vol % acetonitrile (5% AcN), respectively.

We propose the role of nitrogen is as follows. In the presence of pure ethanol, SWNTs grow by the tangential growth mode. The diameters of the SWNTs are therefore similar to the catalyst diameters, which are approximately 2 nm.^{32,54} When nitrogen is introduced into the system, some nitrogen atoms adsorb onto the surface of the catalyst particles. Since N interacts more strongly with the Co nanoparticles than C, the less-mobile N frustrate the formation of the sp² network that is to become the nanotube sidewall. As a result, it becomes difficult to sustain the tangential growth mode, and the perpendicular growth mode becomes energetically favorable. It is possible for the transition between growth modes to be continuous, resulting in SWNT junctions like those shown in Figure 2e,f, but discontinuous growth is more likely. A schematic of this diameter change is shown in Figure 3.

As reported in ref 32, the diameter distribution of Ac-SWNTs is considerably narrow, which is expected for the perpendicular growth mode. While nucleation from different small-diameter catalyst particles is a possible alternative explanation, we expect such small catalyst particles to be quite few in number thus unable to initiate vertically aligned growth (Figure 1a). Synthesis of small-diameter SWNTs from larger catalyst particles *via* the perpendicular mode would result in more SWNTs and would be less sensitive to nanoparticle diameter.

CONCLUSION

We have demonstrated multilayered growth of vertically aligned SWNTs in which the layers have vastly different diameters. Our empirical finding convincingly shows that this diameter change is both reversible and repeatable and suggests that the diameter of substrate-supported SWNTs can be changed *on-demand* without the need to alter catalyst preparation or chemistry. Such growth is also independent of the sequence in which the precursors are introduced. We suggest this diameter reduction is due to nitrogen at the catalyst surface impeding SWNT formation, which causes the growth mode to change from tangential to perpendicular. This change can be continuous, but termination and

renucleation of growth is more likely. The ability to easily and efficiently modulate the nanotube diameter during

SWNT growth is crucial for bottom-up fabrication of carbon nanotube materials and devices.

METHODS

No-flow CVD was employed for synthesis of VA-SWNTs.³⁴ The Co/Mo binary catalysts were prepared as in our previous report.⁵⁵ Pure ethanol (EtOH) and a mixture of 5 vol % of acetonitrile in ethanol (5% AcN) were used as precursor. Catalysts deposited on quartz or silicon substrates were reduced by flowing 300 sccm of Ar/H₂ (3% H₂) during heating (approximately 30 min). After reaching 800 °C, the CVD chamber was evacuated and 40 μ L of a liquid precursor stored in a small cap upstream was introduced by opening a valve. A 5% AcN mixture was first introduced into the reaction chamber for 2 min, after which the CVD chamber was evacuated to base pressure of 27 Pa (approximately 90 s) prior to sealing the CVD chamber and introducing pure EtOH for 90 s. The EtOH supply was finally stopped, and 5% AcN was reintroduced until the growth stopped. The CVD chamber was then immediately cooled under 300 sccm of Ar flow. The actual pressures during EtOH or 5% AcN introduction increased from 1.4 to 2.6 kPa. The growth of VA-SWNTs was monitored *in situ* by a calibrated real-time measurement of the attenuation of a He/Ne (633 nm) laser passing through a quartz substrate supporting the growing films.⁵⁶

The morphology of the resulting multilayered VA-SWNT arrays was imaged by scanning electron microscopy (SEM, 1 kV acceleration voltage, S-4800, Hitachi Co., Ltd). For resonance Raman spectroscopy (Chromex 501is with Andor DV401-Fl), a laser with an excitation wavelength of 488 nm was incident on the cleaved cross-section of the VA-SWNT films using a 50 \times objective lens with a laser power of 0.5 mW. For cross-sectional Raman measurements in Figure 1, the incident laser light was polarized perpendicular to the nanotube axis in order to maximize the contrast of RBM features.⁵⁷

The double-layered sample in which EtOH and 5% AcN were introduced as the first and second feedstocks, respectively, were dispersed in ethanol, and the mean diameter of EtOH- and 5% AcN-grown SWNTs were observed by transmission electron microscopy (TEM, JEOL 2000EX operating at 200 kV). In addition, the as-grown five-layer VA-SWNT array was mildly dispersed in ethanol, and sonicated for a few minutes prior to dropping onto a TEM grid (see Supporting Information). The dispersed five-layer array was observed by high-resolution transmission electron microscope (HRTEM, JEM-ARM200F operated at 200 kV) and low-angle annular dark-field STEM (LAADF-STEM, JEM-2800 operated at 200 kV and detector angle of 34–157 mrad). The CoNTub algorithm⁵⁸ was used to generate the nanotube heterojunction structures for the growth model.

Conflict of Interest: The authors declare no competing financial interest.

Acknowledgment. Part of this work was financially supported by Grants-in-Aid for Scientific Research (22226006, 23760180 and 23760179), JSPS Core-to-Core Program, and the Global COE Program “Global Center for Excellence for Mechanical Systems Innovation”. T.T. acknowledges support from the Higher Educational Strategic Scholarships for Frontier Research Network (CHE-PhD-SFR) granted by the Office of Higher Education Commission, Thailand. C.K. acknowledges the Austrian Academy of Sciences for the APART fellowship A-11456. TEM observation was conducted at the Research Hub for Advanced Nano Characterization, The University of Tokyo, supported by MEXT. The authors acknowledge Prof. Y. Ikuhara of the Institute of Engineering Innovation, School of Engineering for useful comments on TEM images.

Supporting Information Available: SEM images, growth, and resonance Raman spectra of double-layered VA-SWNT arrays. TEM observation of nanotube diameter distribution for double-layered sample. Growth and SEM images of five-layer VA-SWNT

arrays. LAADF-STEM images of dispersed five-layer VA-SWNTs. This material is available free of charge *via* the Internet at <http://pubs.acs.org>.

REFERENCES AND NOTES

1. Bandow, S.; Asaka, S.; Saito, Y.; Rao, A. M.; Grigorian, L.; Richter, E.; Eklund, P. C. Effect of the Growth Temperature on the Diameter Distribution and Chirality of Single-Wall Carbon Nanotubes. *Phys. Rev. Lett.* **1998**, *80*, 3779–3782.
2. Kataura, H.; Kumazawa, Y.; Maniwa, Y.; Ohtsuka, Y.; Sen, R.; Suzuki, S.; Achiba, Y. Diameter Control of Single-Walled Carbon Nanotubes. *Carbon* **2000**, *38*, 1691–1697.
3. Kitiyanan, B.; Alvarez, W. E.; Harwell, J. H.; Resasco, D. E. Controlled Production of Single-Wall Carbon Nanotubes by Catalytic Decomposition of CO on Bimetallic Co–Mo Catalysts. *Chem. Phys. Lett.* **2000**, *317*, 497–503.
4. An, L.; Owens, J. M.; McNeil, L. E.; Liu, J. Synthesis of Nearly Uniform Single-Walled Carbon Nanotubes Using Identical Metal-Containing Molecular Nanoclusters as Catalysts. *J. Am. Chem. Soc.* **2002**, *124*, 13688–13689.
5. Bachilo, S. M.; Balzano, L.; Herrera, J. E.; Pompeo, F.; Resasco, D. E.; Weisman, R. B. Narrow (*n,m*)-Distribution of Single-Walled Carbon Nanotubes Grown Using a Solid Supported Catalyst. *J. Am. Chem. Soc.* **2003**, *125*, 11186–11187.
6. Nasibulin, A. G.; Pikhitsa, P. V.; Jiang, H.; Kauppinen, E. I. Correlation between Catalyst Particle and Single-Walled Carbon Nanotube Diameters. *Carbon* **2005**, *43*, 2251–2257.
7. Chiang, W.-H.; Sankaran, R. M. Linking Catalyst Composition to Chirality Distributions of As-Grown Single-Walled Carbon Nanotubes by Tuning Ni_xFe_{1-x} Nanoparticles. *Nat. Mater.* **2009**, *8*, 882–886.
8. Miyauchi, Y.; Chiashi, S.; Murakami, Y.; Hayashida, Y.; Maruyama, S. Fluorescence Spectroscopy of Single-Walled Carbon Nanotubes Synthesized from Alcohol. *Chem. Phys. Lett.* **2004**, *387*, 198–203.
9. Xiang, R.; Einarsson, E.; Murakami, Y.; Shiomi, J.; Chiashi, S.; Tang, Z.; Maruyama, S. Diameter Modulation of Vertically Aligned Single-Walled Carbon Nanotubes. *ACS Nano* **2012**, *6*, 7472–7479.
10. Wang, B.; Poa, C. H. P.; Wei, L.; Li, L.-J.; Yang, Y.; Chen, Y. (*n,m*) Selectivity of Single-Walled Carbon Nanotubes by Different Carbon Precursors on Co–Mo Catalysts. *J. Am. Chem. Soc.* **2007**, *129*, 9014–9019.
11. Murakami, Y.; Miyauchi, Y.; Chiashi, S.; Maruyama, S. Characterization of Single-Walled Carbon Nanotubes Catalytically Synthesized from Alcohol. *Chem. Phys. Lett.* **2003**, *374*, 53–58.
12. Ago, H.; Imamura, S.; Okazaki, T.; Saito, T.; Yumura, M.; Tsuji, M. CVD Growth of Single-Walled Carbon Nanotubes with Narrow Diameter Distribution over Fe/MgO Catalyst and Their Fluorescence Spectroscopy. *J. Phys. Chem. B* **2005**, *109*, 10035–10041.
13. Ciuparu, D.; Chen, Y.; Lim, S.; Haller, G. L.; Pfefferle, L. Uniform-Diameter Single-Walled Carbon Nanotubes Catalytically Grown in Cobalt-Incorporated MCM-41. *J. Phys. Chem. B* **2004**, *108*, 503–507.
14. Chen, Y.; Ciuparu, D.; Lim, S.; Yang, Y.; Haller, G. L.; Pfefferle, L. Synthesis of Uniform Diameter Single Wall Carbon Nanotubes in Co-MCM-41: Effects of CO Pressure and Reaction Time. *J. Catal.* **2004**, *226*, 351–362.
15. Picher, M.; Anglaret, E.; Arenal, R.; Jourdain, V. Processes Controlling the Diameter Distribution of Single-Walled Carbon Nanotubes during Catalytic Chemical Vapor Deposition. *ACS Nano* **2011**, *5*, 2118–2125.
16. Yao, Y.; Li, Q.; Zhang, J.; Liu, R.; Jiao, L.; Zhu, Y. T.; Liu, Z. Temperature-Mediated Growth of Single-Walled

- Carbon-Nanotube Intramolecular Junctions. *Nat. Mater.* **2007**, *6*, 283–286.
17. Ning, G.; Shinohara, H. Un同步ized Diameter Changes of Double-Wall Carbon Nanotubes during Chemical Vapour Deposition Growth. *Chem. Asian J.* **2009**, *4*, 955–960.
18. Wei, D. C.; Liu, Y. Q.; Cao, L. C.; Fu, L.; Li, X. L.; Wang, Y.; Yu, G.; Zhu, D. B. A New Method to Synthesize Complicated Multibranched Carbon Nanotubes with Controlled Architecture and Composition. *Nano Lett.* **2006**, *6*, 186–192.
19. Ouyang, M.; Huang, J. L.; Lieber, C. M. Fundamental Electronic Properties and Applications of Single-Walled Carbon Nanotubes. *Acc. Chem. Res.* **2002**, *35*, 1018–1025.
20. Jin, Z.; Li, X.; Zhou, W.; Han, Z.; Zhang, Y.; Li, Y. Direct Growth of Carbon Nanotube Junctions by a Two-Step Chemical Vapor Deposition. *Chem. Phys. Lett.* **2006**, *432*, 177–183.
21. Li, J.; Papadopoulos, C.; Xu, J. Nanoelectronics: Growing Y-Junction Carbon Nanotubes. *Nature* **1999**, *402*, 253–254.
22. Meng, G. W.; Jung, Y. J.; Cao, A. Y.; Vajtai, R.; Ajayan, P. M. Controlled Fabrication of Hierarchically Branched Nanopores, Nanotubes, and Nanowires. *Proc. Natl. Acad. Sci. U.S.A.* **2005**, *102*, 7074–7078.
23. Wei, D.; Cao, L.; Fu, L.; Li, X.; Wang, Y.; Yu, G.; Liu, Y. A New Technique for Controllably Producing Branched or Encapsulating Nanostructures in a Vapor–Liquid–Solid Process. *Adv. Mater.* **2007**, *19*, 386–390.
24. Jackson, J. J.; Puretzky, A. A.; More, K. L.; Rouleau, C. M.; Eres, G.; Geohegan, D. B. Pulsed Growth of Vertically Aligned Nanotube Arrays with Variable Density. *ACS Nano* **2010**, *4*, 7573–7581.
25. Geohegan, D. B.; Puretzky, A. A.; Jackson, J. J.; Rouleau, C. M.; Eres, G.; More, K. L. Flux-Dependent Growth Kinetics and Diameter Selectivity in Single-Wall Carbon Nanotube Arrays. *ACS Nano* **2011**, *5*, 8311–8321.
26. Puretzky, A. A.; Geohegan, D. B.; Jackson, J. J.; Pannala, S.; Eres, G.; Rouleau, C. M.; More, K. L.; Thonnard, N.; Readle, J. D. Incremental Growth of Short SWNT Arrays by Pulsed Chemical Vapor Deposition. *Small* **2012**, *8*, 1534–1542.
27. Tian, Y.; Timmermans, M.; Kivistö, S.; Nasibulin, A.; Zhu, Z.; Jiang, H.; Okhotnikov, O.; Kauppinen, E. Tailoring the Diameter of Single-Walled Carbon Nanotubes for Optical Applications. *Nano Res.* **2011**, *4*, 807–815.
28. Zhang, G.; Qi, P.; Wang, X.; Lu, Y.; Mann, D.; Li, X.; Dai, H. Hydrogenation and Hydrocarbonation and Etching of Single-Walled Carbon Nanotubes. *J. Am. Chem. Soc.* **2006**, *128*, 6026–6027.
29. Liu, Q.; Ren, W.; Chen, Z.-G.; Wang, D.-W.; Liu, B.; Yu, B.; Li, F.; Cong, H.; Cheng, H.-M. Diameter-Selective Growth of Single-Walled Carbon Nanotubes with High Quality by Floating Catalyst Method. *ACS Nano* **2008**, *2*, 1722–1728.
30. Yu, B.; Liu, C.; Hou, P.-X.; Tian, Y.; Li, S.; Liu, B.; Li, F.; Kauppinen, E. I.; Cheng, H.-M. Bulk Synthesis of Large Diameter Semiconducting Single-Walled Carbon Nanotubes by Oxygen-Assisted Floating Catalyst Chemical Vapor Deposition. *J. Am. Chem. Soc.* **2011**, *133*, 5232–5235.
31. He, M.; Jiang, H.; Kauppinen, E. I.; Lehtonen, J. Diameter and Chiral Angle Distribution Dependencies on the Carbon Precursors in Surface-Grown Single-Walled Carbon Nanotubes. *Nanoscale* **2012**, *4*, 7394–7398.
32. Thurakitseree, T.; Kramberger, C.; Zhao, P.; Aikawa, S.; Harish, S.; Chiashi, S.; Einarsson, E.; Maruyama, S. Diameter-Controlled and Nitrogen-Doped Vertically Aligned Single-Walled Carbon Nanotubes. *Carbon* **2012**, *50*, 2635–2640.
33. Thurakitseree, T.; Kramberger, C.; Zhao, P.; Chiashi, S.; Einarsson, E.; Maruyama, S. Reduction of Single-Walled Carbon Nanotube Diameter to Sub-nm via Feedstock. *Phys. Status Solidi B* **2012**, *249*, 2404–2407.
34. Xiang, R.; Zhang, Z.; Ogura, K.; Okawa, J.; Einarsson, E.; Miyauchi, Y.; Shiomi, J.; Maruyama, S. Vertically Aligned ¹³C Single-Walled Carbon Nanotubes Synthesized by No-Flow Alcohol Chemical Vapor Deposition and Their Root Growth Mechanism. *Jpn. J. Appl. Phys.* **2008**, *47*, 1971–1974.
35. Kataura, H.; Kumazawa, Y.; Maniwa, Y.; Umezawa, I.; Suzuki, S.; Ohtsuka, Y.; Achiba, Y. Optical Properties of Single-Wall Carbon Nanotubes. *Synth. Met.* **1999**, *103*, 2555–2558.
36. Dresselhaus, M. S.; Dresselhaus, G.; Saito, R.; Jorio, A. Raman Spectroscopy of Carbon Nanotubes. *Phys. Rep.* **2005**, *409*, 47–99.
37. Araujo, P. T.; Doorn, S. K.; Kilina, S.; Tretiak, S.; Einarsson, E.; Maruyama, S.; Chacham, H.; Pimenta, M. A.; Jorio, A. Third and Fourth Optical Transitions in Semiconducting Carbon Nanotubes. *Phys. Rev. Lett.* **2007**, *98*, 067401.
38. Koós, A. A.; Dillon, F.; Obraztsova, E. A.; Crossley, A.; Grobert, N. Comparison of Structural Changes in Nitrogen and Boron-Doped Multi-walled Carbon Nanotubes. *Carbon* **2010**, *48*, 3033–3041.
39. Liu, H.; Zhang, Y.; Li, R.; Sun, X.; Désilets, S.; Abou-Rachid, H.; Jaidann, M.; Lussier, L.-S. Structural and Morphological Control of Aligned Nitrogen-Doped Carbon Nanotubes. *Carbon* **2010**, *48*, 1498–1507.
40. Pfeiffer, R.; Kuzmany, H.; Simon, F.; Bokova, S. N.; Obraztsova, E. Resonance Raman Scattering from Phonon Overtones in Double-Wall Carbon Nanotubes. *Phys. Rev. B* **2005**, *71*, 155409.
41. Cardenas, J. F.; Gromov, A. Double Resonance Raman Scattering in Solubilised Single Walled Carbon Nanotubes. *Chem. Phys. Lett.* **2007**, *442*, 409–412.
42. Zhu, L.; Xiu, Y.; Hess, D. W.; Wong, C.-P. Aligned Carbon Nanotube Stacks by Water-Assisted Selective Etching. *Nano Lett.* **2005**, *5*, 2641–2645.
43. Iwasaki, T.; Zhong, G.; Aikawa, T.; Yoshida, T.; Kawarada, H. Direct Evidence for Root Growth of Vertically Aligned Single-Walled Carbon Nanotubes by Microwave Plasma Chemical Vapor Deposition. *J. Phys. Chem. B* **2005**, *109*, 19556–19559.
44. Iwasaki, T.; Robertson, J.; Kawarada, H. Mechanism Analysis of Interrupted Growth of Single-Walled Carbon Nanotube Arrays. *Nano Lett.* **2008**, *8*, 886–890.
45. Xiang, R.; Einarsson, E.; Okawa, J.; Thurakitseree, T.; Murakami, Y.; Shiomi, J.; Ohno, Y.; Maruyama, S. Parametric Study of Alcohol Catalytic Chemical Vapor Deposition for Controlled Synthesis of Vertically Aligned Single-Walled Carbon Nanotubes. *J. Nanosci. Nanotechnol.* **2010**, *10*, 3901–3906.
46. Ayala, P.; Arenal, R.; Rümmeli, M.; Rubio, A.; Pichler, T. The Doping of Carbon Nanotubes with Nitrogen and Their Potential Applications. *Carbon* **2010**, *48*, 575–586.
47. O’Byrne, J. P.; Li, Z.; Jones, S. L. T.; Fleming, P. G.; Larsson, J. A.; Morris, M. A.; Holmes, J. D. Nitrogen-Doped Carbon Nanotubes: Growth, Mechanism and Structure. *ChemPhysChem* **2011**, *12*, 2995–3001.
48. Hafner, J. H.; Bronikowski, M. J.; Azamian, B. R.; Nikolaev, P.; Rinzler, A. G.; Colbert, D. T.; Smith, K. A.; Smalley, R. E. Catalytic Growth of Single-Wall Carbon Nanotubes from Metal Particles. *Chem. Phys. Lett.* **1998**, *296*, 195–202.
49. Fiawoo, M.-F. C.; Bonnot, A.-M.; Amara, H.; Bichara, C.; Thibault-Pénisson, J.; Loiseau, A. Evidence of Correlation between Catalyst Particles and the Single-Wall Carbon Nanotube Diameter: A First Step Towards Chirality Control. *Phys. Rev. Lett.* **2012**, *108*, 195503.
50. Zhu, W.; Rosen, A.; Bolton, K. Changes in Single-Walled Carbon Nanotube Chirality during Growth and Regrowth. *J. Chem. Phys.* **2008**, *128*, 124708.
51. Hasegawa, K.; Noda, S. Moderating Carbon Supply and Suppressing Ostwald Ripening of Catalyst Particles to Produce 4.5-mm-Tall Single-Walled Carbon Nanotube Forests. *Carbon* **2011**, *49*, 4497–4504.
52. Hofmann, S.; Sharma, R.; Ducati, C.; Du, G.; Mattevi, C.; Cepek, C.; Cantoro, M.; Pisana, S.; Parvez, A.; Cervantes-Sodi, F.; et al. *In situ* Observations of Catalyst Dynamics during Surface-Bound Carbon Nanotube Nucleation. *Nano Lett.* **2007**, *7*, 602–608.
53. Kramberger, C.; Thurakitseree, T.; Koh, H.; Izumi, Y.; Kinoshita, T.; Muro, T.; Einarsson, E.; Maruyama, S. One-Dimensional N₂ Gas inside Single-Walled Carbon Nanotubes. *Carbon* **2013**, *55*, 196–201.
54. Hu, M.; Murakami, Y.; Ogura, M.; Maruyama, S.; Okubo, T. Morphology and Chemical State of Co–Mo Catalysts for Growth of Single-Walled Carbon Nanotubes Vertically Aligned on Quartz Substrates. *J. Catal.* **2004**, *225*, 230–239.

55. Murakami, Y.; Chiashi, S.; Miyauchi, Y.; Hu, M. H.; Ogura, M.; Okubo, T.; Maruyama, S. Growth of Vertically Aligned Single-Walled Carbon Nanotube Films on Quartz Substrates and Their Optical Anisotropy. *Chem. Phys. Lett.* **2004**, *385*, 298–303.
56. Einarsson, E.; Murakami, Y.; Kadokawa, M.; Maruyama, S. Growth Dynamics of Vertically Aligned Single-Walled Carbon Nanotubes from *in Situ* Measurements. *Carbon* **2008**, *46*, 923–930.
57. Zhang, Z.; Einarsson, E.; Murakami, Y.; Miyauchi, Y.; Maruyama, S. Polarization Dependence of Radial Breathing Mode Peaks in Resonant Raman Spectra of Vertically Aligned Single-Walled Carbon Nanotubes. *Phys. Rev. B* **2010**, *81*, 165442.
58. Melchor, S.; Dobado, J. A. CoNTub: An Algorithm for Connecting Two Arbitrary Carbon Nanotubes. *J. Chem. Inf. Comput. Sci.* **2004**, *44*, 1639–1646.